
A Max-Min Entropy Framework for Reinforcement Learning

Seungyul Han

Graduate School of Artificial Intelligence
UNIST
Ulsan, South Korea 44919
syhan@unist.ac.kr

Youngchul Sung[†]

Dept. of Electrical Engineering
KAIST
Daejeon, South Korea 34141
ycsung@kaist.ac.kr

Abstract

In this paper, we propose a max-min entropy framework for reinforcement learning (RL) to overcome the limitation of the soft actor-critic (SAC) algorithm implementing the maximum entropy RL in model-free sample-based learning. Whereas the maximum entropy RL guides learning for policies to reach states with high entropy in the future, the proposed max-min entropy framework aims to learn to visit states with low entropy and maximize the entropy of these low-entropy states to promote better exploration. For general Markov decision processes (MDPs), an efficient algorithm is constructed under the proposed max-min entropy framework based on disentanglement of exploration and exploitation. Numerical results show that the proposed algorithm yields drastic performance improvement over the current state-of-the-art RL algorithms.

1 Introduction

The maximum entropy framework has been considered in various RL domains [22, 23, 30, 45, 51, 53, 58]. Maximum entropy RL adds the expected policy entropy to the return objective of standard RL in order to maximize both the return and the entropy of policy distribution. Maximum entropy RL encourages the policy to choose multiple actions probabilistically and yields a significant improvement in exploration and robustness and good final performance in various control tasks [15, 20, 21, 25, 26, 29, 50]. In particular, soft actor-critic (SAC) implements maximum entropy RL in an efficient iterative manner based on soft policy iteration and guarantees convergence to the optimal policy for finite MDPs, yielding significant performance improvement over various on-policy and off-policy recent RL algorithms in many continuous control tasks. However, we observe that such an iterative implementation of the maximum entropy strategy of optimizing for policies that aim to reach states with high entropy in the future does not necessarily result in the desired exploration behavior but may yield positive feedback hindering exploration in model-free sample-based learning with function approximation. In order to overcome such limitations associated with implementation of the maximum entropy RL, we propose a max-min entropy framework for RL, which aims to learn policies reaching states with low entropy and maximizing the entropy of these low-entropy states, whereas the conventional maximum entropy RL optimizes for policies that aim to visit states with high entropy and maximize the entropy of those high-entropy states for high entropy of the entire trajectory. We implemented the proposed max-min entropy framework into a practical iterative actor-critic algorithm based on policy iteration with disentangled exploration and exploitation. It is demonstrated that the proposed algorithm significantly enhances exploration capability due to the fairness across states induced by the max-min framework and yields drastic performance improvement over existing RL algorithms including maximum-entropy SAC on difficult control tasks.

2 Related Works

Maximum Entropy RL: The maximum entropy framework has been considered in various RL domains: inverse reinforcement learning [58], stochastic optimal control [45, 51, 53], guided policy search [30], and off-policy learning [22, 23]. There is a connection between value-based and policy-based RL under the policy entropy regularization [38], [42] combines them, and finally [46] proves that they are equivalent. Maximum entropy RL is also related to probabilistic inference [40, 45]. Recently, maximizing the entropy of state distribution instead of the policy distribution [26] and maximizing the entropy considering the previous sample action distribution [25] have been investigated for better exploration.

Max-Min Optimization: Max-min optimization aims to maximize the minimum of the objective function [11]. Under the convex-concave assumption, there exist many algorithms to find the solution to a max-min problem by using optimistic mirror descent [44], Frank-Wolfe algorithm [17], and Primal-Dual method [24]. However, non-convex max-min problems are more challenging [37] and there are several recent studies to find (approximate) solutions to non-convex max-min optimization problems [6, 41, 43]. This framework has been used in various optimization/control domains: fair resource allocation [31], inference [4, 56], generative adversarial network (GAN) [2, 18], robust training [33], and reinforcement learning [54].

Exploration in RL: Exploration is one of the most important issues in model-free RL, as there is the key assumption that all state-action pairs must be visited infinitely often to guarantee the convergence of Q -function [55]. In order to explore diverse state-action pairs in the joint state-action space, various methods have been considered in prior works: intrinsically-motivated reward based on curiosity [5, 10], model prediction error [1, 9], information gain [25, 27, 28], and counting states [32, 34]. These exploration techniques improve exploration and performance in challenging sparse-reward environments [3, 9, 12].

3 Background

3.1 Basic RL Setup

We consider an infinite-horizon MDP $(\mathcal{S}, \mathcal{A}, P, \gamma, r)$, where \mathcal{S} is the state space, \mathcal{A} is the action space, P is the transition probability, γ is the discount factor, and r is the bounded reward function. We assume that each action dimension is bounded. The RL agent has a policy $\pi : \mathcal{S} \times \mathcal{A} \rightarrow \mathbb{R}^+ \in \Pi$, which chooses an action a_t for given state s_t according to $a_t \sim \pi(\cdot|s_t)$ at each time step t , where Π is the policy space. For action a_t , the environment yields the reward $r_t := r(s_t, a_t)$ and the next state $s_{t+1} \sim P(s_{t+1}|s_t, a_t)$. Standard RL learns policy π to maximize the discounted return $\mathbb{E}_{s_0 \sim p_0, \tau_0 \sim \pi} [\sum_{t=0}^{\infty} \gamma^t r_t]$, where $\tau_t = (s_t, a_t, s_{t+1}, a_{t+1}, \dots)$ is an episode trajectory.

3.2 Maximum Entropy RL and Soft Actor-Critic

Maximum entropy RL maximizes both the expected return and the expected policy entropy simultaneously to achieve an improvement in exploration and robustness. The entropy-augmented objective function of maximum entropy RL is given by

$$J_{MaxEnt}(\pi) = \mathbb{E}_{s_0 \sim p_0, \tau_0 \sim \pi} \left[\sum_{t=0}^{\infty} \gamma^t (r_t + \alpha \mathcal{H}(\pi(\cdot|s_t))) \right], \quad (1)$$

where $\mathcal{H}(\pi(\cdot|s)) = \mathbb{E}_{a \sim \pi(\cdot|s)} [-\log \pi(a|s)]$ is the entropy function and $\alpha > 0$ is the entropy coefficient. A key point here is that the policy entropy is included in the reward not used as an external regularizer at each time step. Thus, *this maximum entropy RL framework optimizes for policies that aim to reach states on which policies have high entropy in the future* [21].

Soft actor-critic (SAC) is an efficient off-policy actor-critic algorithm to solve the maximum entropy RL problem [22]. SAC maximizes (1) based on soft policy iteration, which consists of soft policy evaluation and soft policy improvement. For this, the soft Q -value of given (s_t, a_t) is defined as

$$Q^\pi(s_t, a_t) := r_t + \mathbb{E}_{\tau_{t+1} \sim \pi} \left[\sum_{l=t+1}^{\infty} \gamma^{l-t} (r_l + \alpha \mathcal{H}(\pi(\cdot|s_l))) \right], \quad (2)$$

which does not include the policy entropy of the current time step but includes the sum of all future policy entropy and the sum of all current and future rewards. For given π , soft policy evaluation guarantees the convergence of soft Q -function estimation, which estimates Q^π by iteratively applying a modified Bellman operator \mathcal{T}^π to a real-valued estimate function $Q : \mathcal{S} \times \mathcal{A} \rightarrow \mathbb{R}$, given by

$$\begin{aligned} \mathcal{T}^\pi Q(s_t, a_t) &= r_t + \gamma \mathbb{E}_{s_{t+1} \sim P(\cdot | s_t, a_t)} [V(s_{t+1})], \quad \text{where} \\ V(s_t) &= \mathbb{E}_{a_t \sim \pi(\cdot | s_t)} [Q(s_t, a_t) - \alpha \log \pi(a_t | s_t)] \end{aligned} \quad (3)$$

and $V(s_t)$ is the soft state value function. Then, at each iteration, SAC updates the policy as

$$\pi_{new} = \arg \min_{\pi \in \Pi} D_{KL} \left(\pi(\cdot | s_t) \parallel \frac{\exp(Q^{\pi_{old}}(s_t, a_t)/\alpha)}{Z^{\pi_{old}}(s_t)} \right) \quad (4)$$

$$= \arg \max_{\pi \in \Pi} \mathbb{E}_{a_t \sim \pi(\cdot | s_t)} [Q^{\pi_{old}}(s_t, a_t) - \alpha \log \pi(a_t | s_t)] \quad (5)$$

where $Z^{\pi_{old}}(s_t)$ is the log partition function which is a function of s_t only. Soft policy improvement guarantees $Q^{\pi_{new}}(s_t, a_t) \geq Q^{\pi_{old}}(s_t, a_t)$ for all $(s_t, a_t) \in \mathcal{S} \times \mathcal{A}$. Finally, soft policy evaluation and soft policy improvement are repeated. Then, any initial policy $\pi \in \Pi$ converges to the optimal policy π^* , i.e., $Q^{\pi^*}(s_t, a_t) \geq Q^{\pi'}(s_t, a_t)$ for all $\pi' \in \Pi$ and all $(s_t, a_t) \in \mathcal{S} \times \mathcal{A}$, and π^* maximizes J_{MaxEnt} [22]. Proof of soft policy iteration assumes finite MDPs. SAC approximates the soft policy iteration by sample-based learning with function approximation in continuous-space cases.

4 Motivation: Limitation of Maximum Entropy SAC in Pure Exploration

In this section, we will consider only the maximum entropy SAC in a pure exploration setup without the reward function (the reward function $r = 0$ in MDPs). As seen in Sec. 3, SAC efficiently solves the maximum entropy RL problem to maximize (1) in an iterative manner based on judiciously-defined state and action value functions and the step-wise optimization cost (5). The well-defined value functions and the local cost function as such enable proof of soft policy improvement for finite MDPs in a similar way to the proof of the classical policy improvement theorem. Note that at each time step, SAC updates the policy to maximize the cost (5), composed of two terms: $\mathbb{E}_{a_t \sim \pi(\cdot | s_t)} [Q^{\pi_{old}}(s_t, a_t)]$ and $\alpha \mathbb{E}_{a_t \sim \pi(\cdot | s_t)} [-\log \pi(a_t | s_t)] = \alpha \mathcal{H}(\pi(a_t | s_t))$. As aforementioned, the soft Q -function contains the sum of current and future rewards and the sum of only future policy entropy. Since we consider only the entropy terms without rewards here, the first term $\mathbb{E}_{a_t \sim \pi(\cdot | s_t)} [Q^{\pi_{old}}(s_t, a_t)]$ is the current estimate of the sum of future entropy when action a_t is taken from policy π at state s_t , whereas the second term $\alpha \mathcal{H}(\pi(a_t | s_t))$ is the entropy of the policy π itself. Hence, at each time step, SAC tries to update the policy π to yield the maximum sum of the estimated future entropy and the policy entropy itself. Here, the term $\mathbb{E}_{a_t \sim \pi(\cdot | s_t)} [Q^{\pi_{old}}(s_t, a_t)]$ plays the role of guiding the policy towards the direction of high future entropy.

Saturation: In sample-based update with function approximation, however, the SAC iteration does not yield the desired result, contrary to the intention behind maximum entropy. To see this, let us consider a pure exploration task in which there is no reward. The considered task is a 100×100 continuous 4-room maze proposed in [25], modified from the continuous grid map available at <https://github.com/huyaoyu/GridMap>. Fig. 1(a) shows the maze environment, where state is the (x, y) -position of the agent in the map, action is (dx, dy) bounded by $[-1, 1] \times [-1, 1]$, and the next state of the agent is $(x + dx, y + dy)$. Starting from the left-lower corner $(0.5, 0.5)$, the agent explores the maze without any external reward. First, note that for this pure exploration task, the optimal policy maximizing $J_{MaxEnt}(\pi)$ is given by the uniform policy that selects all actions in $\mathcal{A} = [-1, 1] \times [-1, 1]$ uniformly regardless of the value of s_t . This is because the uniform distribution has maximum entropy for a bounded space [13]. Then, we compare the exploration behaviour of SAC and the uniform policy in the maze task. Fig. 1(b) shows the mean accumulated number of different visited states averaged over 30 random seeds as time goes, where the shaded region in the curve represents standard deviation (1σ) from the mean and a different state is meant as a nonoverlapping quantized 1×1 square. As seen in Fig. 1(b), SAC explores more states than the uniform policy at the early stage of learning. As learning progresses, however, SAC fails to visit new states after $300k$ time steps, whereas the uniform policy continues visiting new states. As a result, SAC eventually visits fewer states than the uniform policy on average. The result shows that SAC fails to converge to the optimal uniform policy and its performance become saturated.

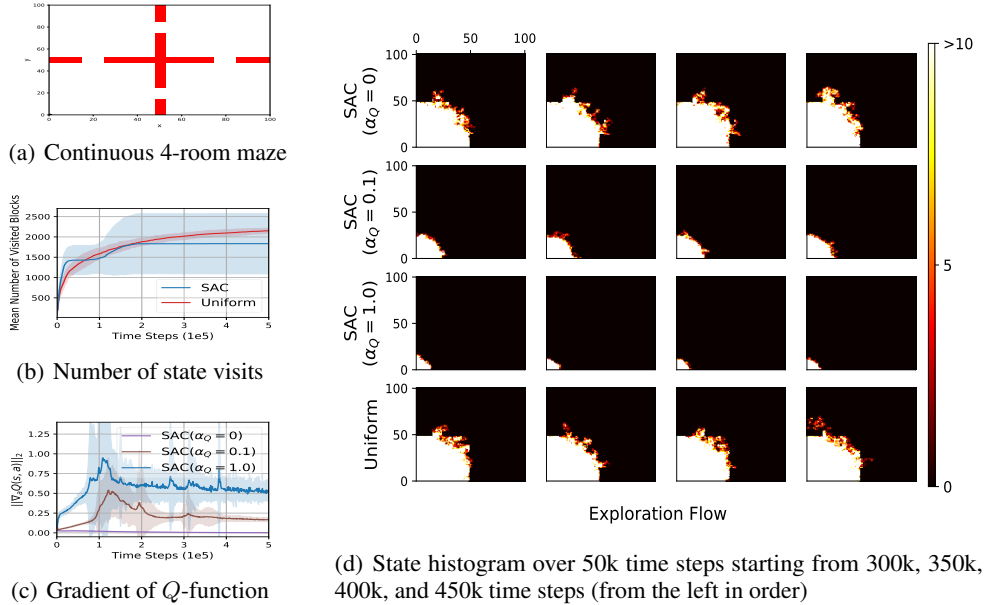


Figure 1: Comparison of SAC and the uniform policy in the continuous 4-room maze

Narrow Exploration Radius: To examine the saturation behavior of SAC in the above pure exploration task, we investigate the policy update of SAC in (5). Since the current Q -function estimate (implemented by a neural network) replaces $Q^{\pi^{old}}$ in (5) in implementation with function approximation, the policy update is rewritten as

$$\arg \max_{\pi \in \Pi} \{ \mathbb{E}_{a_t \sim \pi(\cdot|s_t)} [Q(s_t, a_t)] + \alpha \mathcal{H}(\pi(\cdot|s_t)) \}. \quad (6)$$

As mentioned already, the first term $\mathbb{E}_{a_t \sim \pi(\cdot|s_t)} [Q(s_t, a_t)]$ is the current estimate of the sum of future entropy in this pure exploration case when action a_t is taken from policy π at state s_t , whereas the second term $\alpha \mathcal{H}(\pi(a_t|s_t))$ is the entropy of the policy π itself. The first term $\mathbb{E}_{a_t \sim \pi(\cdot|s_t)} [Q(s_t, a_t)]$ intends to direct the policy towards the direction of high future entropy. Note that maximizing the second term already yields the uniform policy, but the Q -function term affects the policy update. In order to see how the Q -function term actually affects the policy update, we differentiate the entropy coefficient α in the policy update part (5) or (6) as the policy entropy coefficient α_π and that in the soft value function part (2) and (3) as the value entropy coefficient α_Q . We fix α_π as $\alpha_\pi = 1$ and change α_Q as 0, 0.1, and 1 (note that the case of $\alpha_Q = 1$ is original SAC). With this change of α_Q , we conducted the same pure exploration maze task. Fig. 1(c) shows the average norm of the gradient of Q -function with respect to action, i.e., $\mathbb{E}_{s_t \sim \mathcal{D}} [\|\nabla_a Q(s_t, a)|_{a=a_t}\|]$ over time with $a_t \sim \pi(\cdot|s_t)$ and s_t from a mini-batch drawn from the replay buffer \mathcal{D} of SAC update, where the Q neural network weights were initialized randomly. Fig. 1(d) shows the histogram of states that the policy visits over 50k time steps starting from 300k, 350k, 400k, and 450k time steps. When $\alpha_Q = 0$ with no reward, the Q -function update by the Bellman operator \mathcal{T}^π in (3) is trivial as $Q(s, a) \leftarrow \mathbb{E}_{s' \sim P(\cdot|s, a), a' \sim \pi(\cdot|s')} [Q(s', a')]$, i.e., replacement. When the initial $Q(s, a)$ is (nearly) flat over $\mathcal{S} \times \mathcal{A}$ by initial random weight assignment for the Q -neural network, the flat Q is maintained by this trivial update. Indeed, it is seen in Fig. 1(c) that $\mathbb{E}_{s_t \sim \mathcal{D}} [\|\nabla_a Q(s_t, a)|_{a=a_t}\|]$ with $a_t \sim \pi(\cdot|s_t)$ is nearly zero across all time for $\alpha_Q = 0$. With a flat function $Q(s_t, \cdot) \approx c$ over the action space \mathcal{A} , the first term $\mathbb{E}_{a_t \sim \pi(\cdot|s_t)} [Q(s_t, a_t)]$ in (6) does not affect the policy update, only the second term $\mathcal{H}(\pi(\cdot|s_t))$ works, and thus the policy update yields π to converge to the uniform policy for every state maximizing the total entropy. Hence, the exploration radius in the case of $\alpha_Q = 0$ is almost the same as that of the uniform policy, as seen in Fig. 1(d). When $\alpha_Q > 0$, on the other hand, the Q -function starts to be updated nontrivially by the Bellman operator \mathcal{T}^π in (3) due to the $-\log \pi(a_{t+1}|s_{t+1})$ term in $V(s_{t+1})$ in (3), with π given by the current policy. It is now seen in Fig. 1(c) that $\mathbb{E}_{s_t \sim \mathcal{D}} [\|\nabla_a Q(s_t, a)|_{a=a_t}\|]$ is not zero anymore and the gradient norm becomes larger as α_Q increases from 0.1 to 1.0. Non-zero $\mathbb{E}_{s_t \sim \mathcal{D}} [\|\nabla_a Q(s_t, a)|_{a=a_t}\|]$ means that $Q(s_t, \cdot)$ as a function of action a_t for given s_t is not flat anymore and the first term in (6) affects the policy update so that the policy is updated for the direction of high Q -value (with intention for high future entropy) as well

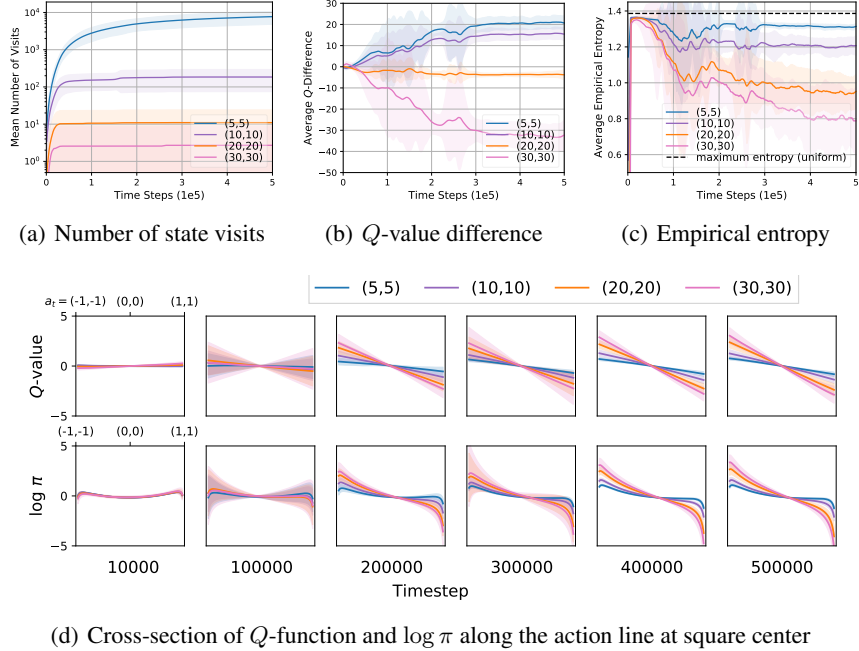


Figure 2: Analysis on sample trajectories of SAC in the continuous maze task

as high policy entropy $\mathcal{H}(\pi)$. As seen in Fig. 1(d), however, the exploration radius reduces as α_Q increases from 0 to 1. The iteration process does not evolve for wider exploration as intended.

5 Methodology

5.1 A Deeper Look at Pure Exploration

In order to propose our new approach overcoming the limitation of SAC implementation of the maximum entropy framework, we first take a deeper look at how the Q -function term in (6) hinders exploration, as SAC (with $\alpha_\pi = \alpha_Q = 1$) learns the maze task. For this, we consider four 2×2 squares centered at $(5, 5)$, $(10, 10)$, $(20, 20)$, and $(30, 30)$ in the 100×100 maze, where every episode starts from $(0.5, 0.5)$. Fig. 2(a) shows the number of accumulated visits to each square as time elapses. Figs. 2(b) and 2(c) show the estimated Q value and the average empirical entropy of each square, respectively, as time goes. For Fig. 2(b), every 1000 time steps, we sampled 1000 states uniformly from each square and an action from the current policy for each sampled state, and computed the Q -value average over the 1000 state-action samples for each square. Then, we computed the mean value of the four average values of the four squares. Fig. 2(b) shows the average Q value of each square relative to the four-square mean value as time goes. For Fig 2(c), every 1000 time steps, we sampled 1000 states uniformly from each square and computed the average empirical entropy $\mathbb{E}_{s_t} [\mathbb{E}_{a_t \sim \pi(\cdot|s_t)} [-\log \pi(a_t|s_t)]]$ of the current policy π at time t averaged over the 1000 sampled states $\{s_t\}$ from each square. The upper row of Fig. 2(d) shows the cross-section of the estimate Q -function $Q(s, a)$ along the diagonal action line from $(-1, -1)$ to $(1, 1)$ at the center state s of each square, as time goes, where each curve is shifted in y -axis so that the mean value averaged over samples along the action line is matched to zero in y -axis. The lower row of Fig. 2(d) shows the value of $\log \pi(a|s)$ of the current policy π at time step t along the diagonal action line from $(-1, -1)$ to $(1, 1)$ at the center state s for each square as time goes, where the curve is shifted in y -axis to match the mean value to zero in y -axis.

First, note from Fig. 2(a) that the farther a state is from the starting point $(0.5, 0.5)$, the less the agent visits the state, and the visitation difference is large. At the early stage of learning starting with random Q -network weight initialization and random policy-network weight initialization, there is little Q -value difference with respect to either state or action, as seen in Figs. 2(b) and 2(d), so the entropy term is dominant in the policy update (6) and the policy entropy increases with the policy

distribution approaching the uniform distribution, as seen in Fig. 2(c). As time goes, learning of the Q -function with the Bellman backup (3) progresses. Basically, the Bellman backup (3) with no reward adds $\Delta Q_t = \gamma\{\mathbb{E}_{a_{t+1}\sim\pi(\cdot|s_{t+1})}[Q(s_{t+1}, a_{t+1})] + \alpha\mathcal{H}(\pi(\cdot|s_{t+1}))\} - Q(s_t, a_t)$ to $Q(s_t, a_t)$ for every $(s_t, a_t) \in \mathcal{S} \times \mathcal{A}$. However, this is approximated in practical RL. In sample-based off-policy learning with function approximation, RL typically stores visited state-action pairs in the replay buffer \mathcal{D} and the above Bellman backup is approximated as updating the Q -function by minimizing the loss $\mathbb{E}_{(s_t, a_t)\sim\mathcal{D}}[(Q(s_t, a_t) - Q^{target}(s_t, a_t))^2]$ based on a mini-batch uniformly drawn from the buffer. Under this off-policy learning with experience replay, when the initial Q -function is roughly flat and small, ΔQ_t soon becomes positive (the policy update increases the entropy of the visited states and ΔQ_t soon becomes positive for the visited states), and hence the Q -values of frequently-visited states are updated more and thus have higher Q -values as seen in Fig.2(b). This is because these states are stored more into \mathcal{D} and sampled more from \mathcal{D} at mini-batch generation. Then, the initial Q -value difference biases the policy to visit the states with high Q -values more frequently than the states with low Q -values because the policy is updated to choose actions that maximizes the expectation of Q -value $\mathbb{E}_{a_t\sim\pi(\cdot|s_t)}[Q(s_t, a_t)]$ in the policy update (6). This is evident in the Fig. 2(d), which shows the estimate of Q -function and the value of $\log \pi$ along the diagonal line. At the early stage of learning (10k time step in the figure), Q -function is roughly flat and the policy is almost close to the uniform distribution for the action line. As the time steps go on, the Q -values of actions close to $(-1, -1)$ becomes higher than the Q -value of actions near $(1, 1)$ due to the off-policy learning with experience replay, as explained above. Then, the policy is updated to choose actions with high Q -values more frequently to maximize the Q -value expectation, so the probability of choosing action $(-1, -1)$ towards the left-lower corner becomes higher than that of action $(1, 1)$ for the opposite direction. As the policy distribution leans toward a certain action and becomes asymmetric away from uniformity, the policy entropy decreases further. As seen in Fig. 2(c), the speed of the policy entropy decrease varies depending on the Q -value difference along the action line in Fig. 2(d), and the policy entropy difference deepens the Q -value difference between states in Fig. 2(b) because the Q -value estimates the policy entropy sum of future states. This positive feedback continues until saturation, as seen in Fig. 2(b), and it results in the narrow exploration radius in Fig. 1(d) because the policy will be forced to visit states with high Q -values only. Note that this positive feedback reduces the policy entropy due to the Q -value difference, contrary to the intention behind maximum entropy.

5.2 Max-Min Entropy RL

In order to break the unwanted positive feedback loop occurring when implementing the maximum entropy framework (i.e., max-max entropy framework) in the previous subsection, we must reduce the policy entropy difference between states to reduce the Q -value difference between states in the feedback loop. For this, we aim to learn the Q -function so that the policy visits states with low entropy, and the policy update increases the policy entropy of these low-entropy states. Under this principle, we propose a new max-min entropy (MME) framework that aims to learn the Q -function to estimate the negative sum of policy entropy, while maintaining the policy entropy maximization term $\mathcal{H}(\pi(\cdot|s_t))$ in the policy update to increase the policy entropy of the visited states. Thus, we define the reversed soft Q -function $Q_R^\pi(s_t, a_t)$ for MME as

$$Q_R^\pi(s_t, a_t) := r_t + \mathbb{E}_{\tau_{t+1}\sim\pi} \left[\sum_{l=t+1}^{\infty} \gamma^{l-t} (r_l - \alpha_Q \mathcal{H}(\pi(\cdot|s_l))) \right], \quad (7)$$

whereas the original soft Q -function of SAC in (2) is given by

$$Q^\pi(s_t, a_t) := r_t + \mathbb{E}_{\tau_{t+1}\sim\pi} \left[\sum_{l=t+1}^{\infty} \gamma^{l-t} (r_l + \alpha_\pi \mathcal{H}(\pi(\cdot|s_l))) \right].$$

Note that the original soft Q -function Q^π adds the policy entropy to the reward and drives the policy to visit states with high entropy. On the other hand, our reversed soft Q -function subtracts the policy entropy from the reward and drives the policy to visit states with low entropy. In this sense, we call Q_R as the ‘‘reversed’’ soft Q -function because it desires the reverse behavior of soft Q -function.

Then, Q_R^π is estimated by a real-valued function $Q_R : \mathcal{S} \times \mathcal{A} \rightarrow \mathbb{R}$ based on a Bellman operator \mathcal{T}_R^π :

$$\mathcal{T}_R^\pi Q_R(s_t, a_t) = r_t + \gamma \mathbb{E}_{s_{t+1}\sim P(\cdot|s_t, a_t)} [V_R(s_{t+1})], \quad (8)$$

where $V_R(s_t) = \mathbb{E}_{a_t \sim \pi(\cdot|s_t)}[Q_R(s_t, a_t) + \alpha_Q \log \pi(a_t|s_t)]$ is the reversed soft state value function. At each iteration, the policy of MME is updated as

$$\pi_{new} = \arg \max_{\pi \in \Pi} \mathbb{E}_{a_t \sim \pi(\cdot|s_t)}[Q_R^{\pi, old}(s_t, a_t) - \alpha_\pi \log \pi(a_t|s_t)], \quad (9)$$

where $Q_R^{\pi, old}$ is substituted by the estimate function Q_R at the iteration. Then, in pure exploration with no reward $r_t = 0, \forall t$, the policy of MME will visit the states with low entropy due to the first term $\mathbb{E}_{a_t \sim \pi(\cdot|s_t)}[Q_R^{\pi, old}(s_t, a_t)]$, and the policy entropy of those states will increase by the second term $\mathbb{E}_{a_t \sim \pi(\cdot|s_t)}[-\log \pi(a_t|s_t)] = \mathcal{H}(\pi(\cdot|s_t))$, as we intended. Note that the behaviour of the proposed method follows the max-min principle [11], so we expect that our MME fairly increase the policy entropy of all states based on the fairness perspective of max-min optimization, whereas SAC increases the policy entropy of states with high entropy only. The MME is expected to reduce the entropy difference and the Q -value difference between states to reduce the unwanted feedback loop and solve the saturation problem. Furthermore, SAC considers the same entropy coefficient α_π for its policy update and the soft Q -function Q^π , but our MME distinguishes the policy entropy coefficient α_π in the policy update (9) and the value-entropy coefficient α_Q in the reversed soft Q -function Q_R^π in (7), as we experimented in Section 4. Changing α_Q and α_π allows for us to control the amount of the reversed Q -function in the policy update, and it will determine the ratio between the exploration due to the policy entropy and the exploration due to the reversed soft Q -function.

In actual implementation, the negative entropy in (7) is plus-offsetted to make the Q -update increase the Q -value. The detailed implementation and algorithm of MME are provided in Appendix A.

5.3 Disentangled Exploration and Exploitation for Rewarded Setup

In the previous subsection, we considered the problem from a pure exploration perspective. However, the ultimate goal of RL is to maximize the sum of rewards in rewarded environments, and the goal of exploration is to receive higher rewards without falling into local optima. With non-zero reward in (7) - (9), the policy will not only visit states with low entropy but also states with higher return. In this case, the reward and the entropy are intertwined in the Q -function and then it is difficult to expect the intended MME exploration behavior through the intertwined Q -function. Therefore, we disentangle exploration from exploitation for rewarded setup, as considered in several previous works [7, 49], and propose disentangled MME (DE-MME) for rewarded setup. For this, we consider two policies: pure exploration policy π_E that samples actions for pure exploration as described in Sec. 5.2, and target policy π_T that actually interacts with the environment. We decompose the reversed soft Q -function Q_R^π in (7) into two terms $Q_R^\pi = Q_{R,R}^\pi + Q_{R,E}^\pi$, where $Q_{R,R}^\pi$ is the expected current and future reward sum considered in standard RL and $Q_{R,E}^\pi$ is the expected sum of future entropy:

$$Q_{R,R}^\pi(s_t, a_t) = r_t + \mathbb{E}_{\tau_{t+1} \sim \pi} \left[\sum_{l=t+1}^{\infty} \gamma^{l-t} r_l \right], Q_{R,E}^\pi(s_t, a_t) = -\alpha_Q \mathbb{E}_{\tau_{t+1} \sim \pi} \left[\sum_{l=t+1}^{\infty} \gamma^{l-t} \mathcal{H}(\pi(\cdot|s_t)) \right].$$

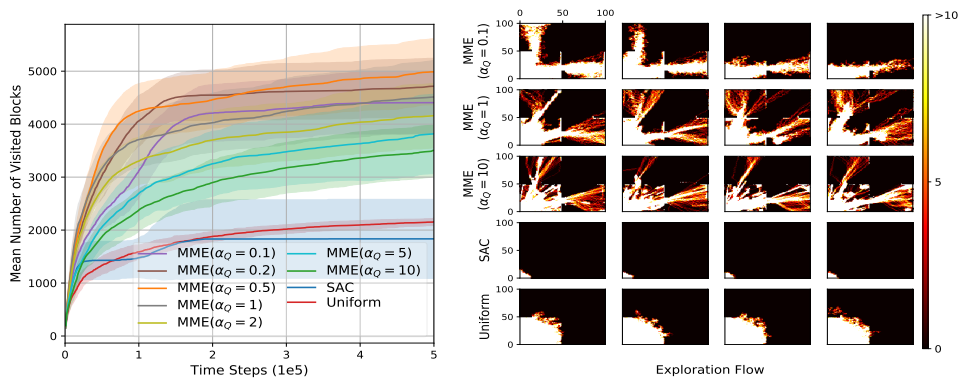
Then, we update the policy π_E for pure exploration as

$$\pi_{E, new} = \arg \max_{\pi' \in \Pi} \mathbb{E}_{a_t \sim \pi'(\cdot|s_t)} \left[Q_{R,E}^{\pi', old}(s_t, a_t) - \alpha_\pi \log \pi'(a_t|s_t) \right]. \quad (10)$$

Note that increasing the expectation of $Q_{R,E}^{\pi', old}$ makes the policy visit states with low entropy of π_E , as we intended in the pure exploration case in Sec. 5.2. Finally, we update the target policy π_T by using $Q_{R,E}^{\pi', old}$ as

$$\pi_{T, new} = \arg \max_{\pi' \in \Pi} \mathbb{E}_{a_t \sim \pi'(\cdot|s_t)} \left[Q_{R,R}^{\pi', old}(s_t, a_t) + Q_{R,E}^{\pi', old}(s_t, a_t) - \alpha_\pi \log \pi'(a_t|s_t) \right]. \quad (11)$$

For implementation, $Q_{R,R}^{\pi', old}$ and $Q_{R,E}^{\pi', old}$ are estimated by real-valued functions $Q_{R,R}$ and $Q_{R,E}$ based on their own Bellman operators (see Appendix A). Note that the policy update (9) in Sec. 5.2 can be expressed as maximizing $\mathbb{E}_{a_t \sim \pi'(\cdot|s_t)}[Q_R^{\pi', old}(s_t, a_t) - \alpha_\pi \log \pi'(a_t|s_t)]$ over the target policy, where $Q_R^{\pi', old} = Q_{R,R}^{\pi', old} + Q_{R,E}^{\pi', old}$. Thus, we can view that the policy update in (11) replaces $Q_R^{\pi', old}$ in the previous policy update (9) with $Q_{R,E}^{\pi', old}$ to disentangle exploration from exploitation. In this way, the policy update (11) will simultaneously increase the expectation of $Q_{R,R}^{\pi', old}$ to maximize the reward sum, the expectation of $Q_{R,E}^{\pi', old}$ to visit states with low entropy, and the policy entropy for diverse action. The detailed implementation and algorithm for DE-MME are provided in Appendix A.



(a) Number of visited states (b) State histogram of every 50k steps after 300k steps

Figure 3: Comparison of MME (Proposed), SAC, and the uniform policy in the 4-room maze

6 Experiments

We provide numerical results to show the performance of the proposed MME and DE-MME in pure exploration and various control tasks. We provide source code for the proposed method at <http://github.com/seungyulhan/mme/> that requires Python Tensorflow. For all plots, the solid line represents the mean over random seeds and the shaded region represents 1 standard deviation from the mean.

6.1 Pure Exploration

To see how the proposed method behaves in pure exploration, we considered the maze task described in Sec.4 again. We compared the exploration performance of MME in Sec.5.2, SAC, and the uniform policy. For MME, we considered several $\alpha_Q \in \{0.1, 0.2, 0.5, 1, 2, 5, 10\}$ with $\alpha_\pi = 1$. Fig. 3(a) in the next page shows the mean number of accumulated quantized visited states averaged over 30 random seeds corresponding to Fig. 1(b), and Fig. 3(b) shows the histogram of visited states, of which setup is the same as Fig.1(d). As seen in Fig. 3(a), the proposed MME visits much more states than SAC or the uniform policy. In addition, we observe that MME continues discovering new states throughout the learning, while SAC rarely visits new states as learning progresses. As seen in Fig. 3(b), MME explores far and rare states as compared to SAC or the uniform policy, and this leads to a large enhancement in exploration performance, as intended in Sec. 5.2. Note that the larger α_Q in update (7) (9) with $r_t = 0$, the stronger is the effect of the Q -function term to visit states with low entropy and the weaker is the effect of the policy entropy term to explore widely in the action space, as we expected in Section 5.2. Hence, there is a trade-off between the two terms and $\alpha_Q = 0.5$ seems best in the maze task when $\alpha_\pi = 1.0$, as seen in Fig. 3(a). Thus, the result clearly shows why we distinguish the policy entropy coefficient α_π and the value entropy coefficient α_Q for MME, whereas SAC uses the common entropy coefficient $\alpha = \alpha_\pi = \alpha_Q$. We also plotted the Q -value difference and the empirical entropy of the four squares centered at (5,5), (10,5), (20,5) and (30,5) for MME, as done in Figs. 2(b) and 2(c). The result is shown in Fig. 4. It is seen that the Q -value difference and the entropy difference among the states are clearly reduced as compared to Figs. 2(b) and 2(c). It means that MME breaks the unwanted positive feedback loop and improves the policy entropy of diverse states more uniformly as compared to SAC in terms of fairness under our max-min framework. This leads to better exploration, as seen in Fig 3.

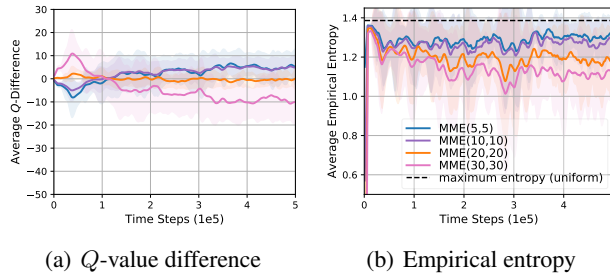


Figure 4: Performance of MME

As seen in Fig. 3(a), the proposed MME visits much more states than SAC or the uniform policy. In addition, we observe that MME continues discovering new states throughout the learning, while SAC rarely visits new states as learning progresses. As seen in Fig. 3(b), MME explores far and rare states as compared to SAC or the uniform policy, and this leads to a large enhancement in exploration performance, as intended in Sec. 5.2. Note that the larger α_Q in update (7) (9) with $r_t = 0$, the stronger is the effect of the Q -function term to visit states with low entropy and the weaker is the effect of the policy entropy term to explore widely in the action space, as we expected in Section 5.2. Hence, there is a trade-off between the two terms and $\alpha_Q = 0.5$ seems best in the maze task when $\alpha_\pi = 1.0$, as seen in Fig. 3(a). Thus, the result clearly shows why we distinguish the policy entropy coefficient α_π and the value entropy coefficient α_Q for MME, whereas SAC uses the common entropy coefficient $\alpha = \alpha_\pi = \alpha_Q$. We also plotted the Q -value difference and the empirical entropy of the four squares centered at (5,5), (10,5), (20,5) and (30,5) for MME, as done in Figs. 2(b) and 2(c). The result is shown in Fig. 4. It is seen that the Q -value difference and the entropy difference among the states are clearly reduced as compared to Figs. 2(b) and 2(c). It means that MME breaks the unwanted positive feedback loop and improves the policy entropy of diverse states more uniformly as compared to SAC in terms of fairness under our max-min framework. This leads to better exploration, as seen in Fig 3.

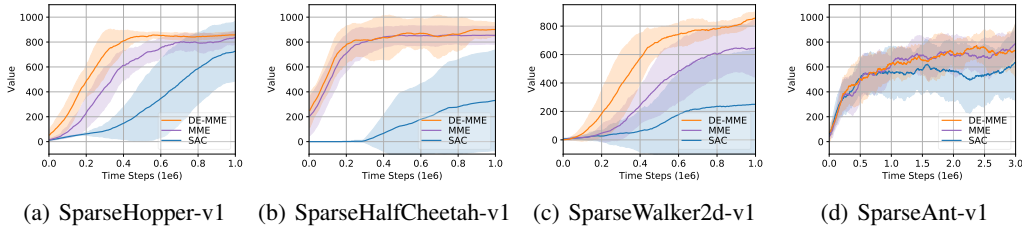


Figure 5: Performance comparison on Sparse Mujoco tasks

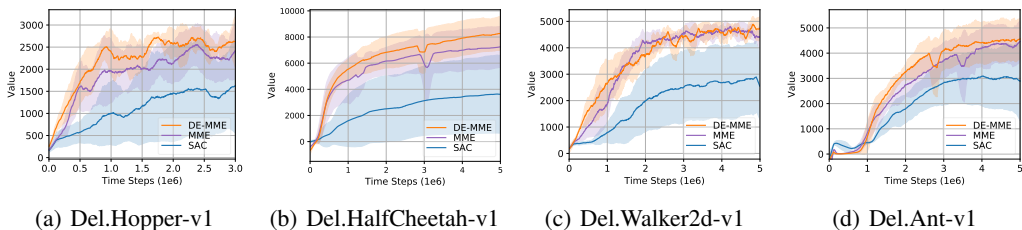


Figure 6: Performance comparison on Delayed Mujoco tasks

6.2 Performance in Rewarded Environments

As mentioned in Sec.5.3, the ultimate goal of RL is to maximize the reward sum in rewarded environments and exploration is one of the means to achieve this goal. Based on the enhanced exploration performance of MME, we expect MME/DE-MME to show good performance in rewarded environments too. In order to verify this, we considered three types of difficult control tasks for which current state-of-the-art RL algorithms do not show satisfactory performance: Two types of sparse-reward tasks (SparseMujoco tasks and DelayedMujoco tasks) and high dimensional Humanoid tasks. SparseMujoco [27, 35] is a sparse version of Mujoco [52] in OpenAI Gym [8], and the reward is 1 if the agent crosses the x -axis threshold τ , otherwise 0. DelayedMujoco [19, 57] is a delayed version of Mujoco in which the reward is accumulated for D time steps and the agent receives the accumulated reward sum once every D time steps. During the accumulation time, the agent receives no reward. These sparse-reward environments have widely been considered as challenging environments for validating the performance of exploration in many previous works [9, 25, 27].

First, we compared the performance of MME algorithms to that of maximum entropy SAC in the sparse-reward tasks. For MME, we considered two versions: vanilla MME proposed in Sec.5.2, and disentangled MME (DE-MME) proposed in Sec.5.3. For MME/DE-MME, we fixed α_π of MME and DE-MME to be equal to α of SAC, and chose proper α_Q for each task. Detailed experimental setup is provided in Appendix B. Figs. 5 and 6 show the performance averaged over 10 random seeds on SparseMujoco tasks and 5 random seeds on DelayedMujoco tasks, respectively. It is seen that the proposed MME shows much higher performance than SAC in the considered environments with rewards. It is also seen that MME itself performs well enough in most environments but DE-MME indeed yields performance gain over vanilla MME and the gain is large in SparseWalker. Thus, disentanglement of exploration from exploitation is beneficial to MME for better reward performance in rewarded environments, as discussed in Sec.5.3. We provided the corresponding max average return tables in Appendix C and ablation study for further analysis in Appendix D. There, one of ablation study empirically shows that the performance enhancement by MME is caused by improved exploration of MME as we intended.

Finally, we compared the performance of MME/DE-MME to that of popular general RL algorithms and recent exploration methods on the considered sparse-reward environments (SparseMujoco and DelayedMujoco tasks) and dense-reward high-dimensional Mujoco tasks (Humanoid, Humanoid-Standup). We considered several action-based exploration methods: SAC combined with divergence [27] (SAC-Div) and diversity actor-critic (DAC) [25], and state-based exploration methods with random network distillation (RND) [9] and MaxEnt (State) [26]. For general RL algorithms, we considered several on-policy RL algorithms: proximal policy optimization (PPO) [48] and trust-region policy optimization (TRPO) [47], and entropy-based off-policy RL algorithms: soft Q-learning (SQL) [21] and SAC [22]. We provided detailed explanation and implementation for each algorithm in

Appendix C. Table 1 summarizes the max average return result. It is seen that MME/DE-MME have superior performance to other methods.

	MME	DE-MME	DAC	SAC-Div	RND	MaxEnt(State)
Sps.Hopper	902.50±4.36	893.30±6.72	900.30±3.93	817.40±253.54	897.90±6.06	879.50±30.96
Sps.HalfCheetah	903.50±34.97	924.90±39.57	915.90±50.71	394.70±405.53	827.80±85.61	924.70±24.44
Sps.Walker2d	818.00±208.60	886.60±25.77	665.10±355.66	278.50±398.23	750.90±179.09	705.30±274.88
Sps.Ant	953.70±28.39	973.60±12.55	935.80±37.08	870.70±121.14	920.60±107.50	940.70±43.84
Del. Hopper	3421.32±88.29	3435.28±39.55	3428.18±69.08	2090.64±1383.83	2721.06±1199.20	3254.10±30.75
Del. HalfCheetah	7299.28±1562.19	8451.20±1375.27	7594.70±1259.23	4080.67±3418.07	7429.94±1383.75	7907.98±535.41
Del. Walker2d	5148.58±193.78	5274.89±186.35	4067.11±257.81	4048.11±290.48	4098.63±683.36	4430.61±347.02
Del. Ant	4664.04±836.37	4851.64±830.88	4243.19±795.49	3978.34±1370.23	1361.36±704.69	1156.61±112.40
	MME	DE-MME	SAC	SQL	PPO	TRPO
Humanoid- Standup	267734.03 ±74302.99	250935.53 ±49386.43	167394.36 ±7291.99	138996.84 ±33903.03	160211.90 ±3268.37	153919.84 ±1575.62
Humanoid	9080.54±768.52	8607.75±570.61	6760.81±267.78	5010.72±248.59	6153.54±246.95	5730.74±455.90

Table 1: Max average return of MME/DE-MME and other recent RL algorithms

7 Conclusion

In this paper, we have proposed a MME framework for RL to resolve the unwanted exploration behavior of maximum entropy RL in off-policy learning with function approximation. In pure exploration, to implement MME, we train the Q -function to visit states with low entropy contrary to the maximum entropy strategy, while maintaining the policy entropy maximization term in the policy update. Then, we extended MME to rewarded environments. In rewarded environments we disentangle exploration from exploitation for MME to explore diverse states as in pure exploration as well as to achieve high return. Numerical results show that the proposed MME explores farther and wider in the state space than maximum entropy realization, alleviates possible positive feedback of off-policy maximum entropy learning, and yields a significant enhancement in exploration and final performance over existing RL methods in various difficult tasks. As for potential impacts, RL can be applied to sensitive areas that require control, such as drone control. However, it is only a risk that RL itself has, and it is not very relevant to the work that we are trying to address in this paper.

8 Acknowledgement

This work is supported by Center for Applied Research in Artificial Intelligence (CARAI) grant funded by Defense Acquisition Program Administration (DAPA) and Agency for Defense Development (ADD) (UD190031RD). Dr. Seungyul Han is currently with AI Graduate School of UNIST and his work is partly supported by Artificial Intelligence Graduate School support (UNIST), Institute of Information & Communications Technology Planning & Evaluation (IITP) grant funded by the Korea government (MSIT) (No.2020-0-01336).

References

- [1] Joshua Achiam and Shankar Sastry. Surprise-based intrinsic motivation for deep reinforcement learning. *arXiv preprint arXiv:1703.01732*, 2017.
- [2] Martin Arjovsky, Soumith Chintala, and Léon Bottou. Wasserstein generative adversarial networks. In *International conference on machine learning*, pages 214–223. PMLR, 2017.
- [3] Adrià Puigdomènech Badia, Pablo Sprechmann, Alex Vitvitskyi, Daniel Guo, Bilal Piot, Steven Kapturowski, Olivier Tieleman, Martín Arjovsky, Alexander Pritzel, Andrew Bolt, et al. Never give up: Learning directed exploration strategies. *arXiv preprint arXiv:2002.06038*, 2020.
- [4] Sina Baharlouei, Maher Nouiehed, Ahmad Beirami, and Meisam Razaviyayn. R\`enyi fair inference. *arXiv preprint arXiv:1906.12005*, 2019.
- [5] Gianluca Baldassarre and Marco Mirolli. *Intrinsically motivated learning in natural and artificial systems*. Springer, 2013.
- [6] Babak Barazandeh and Meisam Razaviyayn. Solving non-convex non-differentiable min-max games using proximal gradient method. In *ICASSP 2020-2020 IEEE International Conference on Acoustics, Speech and Signal Processing (ICASSP)*, pages 3162–3166. IEEE, 2020.
- [7] Lucas Beyer, Damien Vincent, Olivier Teboul, Sylvain Gelly, Matthieu Geist, and Olivier Pietquin. Mulex: Disentangling exploitation from exploration in deep rl. *arXiv preprint arXiv:1907.00868*, 2019.
- [8] Greg Brockman, Vicki Cheung, Ludwig Pettersson, Jonas Schneider, John Schulman, Jie Tang, and Wojciech Zaremba. Openai gym. *arXiv preprint arXiv:1606.01540*, 2016.
- [9] Yuri Burda, Harrison Edwards, Amos Storkey, and Oleg Klimov. Exploration by random network distillation. *arXiv preprint arXiv:1810.12894*, 2018.
- [10] Nuttapon Chentanez, Andrew G Barto, and Satinder P Singh. Intrinsically motivated reinforcement learning. In *Advances in neural information processing systems*, pages 1281–1288, 2005.
- [11] Altannar Chinchuluun, Panos M Pardalos, Athanasios Migdalas, and Leonidas Pitsoulis. *Pareto optimality, game theory and equilibria*. Springer, 2008.
- [12] Jongwook Choi, Yijie Guo, Marcin Moczulski, Junhyuk Oh, Neal Wu, Mohammad Norouzi, and Honglak Lee. Contingency-aware exploration in reinforcement learning. *arXiv preprint arXiv:1811.01483*, 2018.
- [13] Thomas M Cover. *Elements of information theory*. John Wiley & Sons, 1999.
- [14] Prafulla Dhariwal, Christopher Hesse, Oleg Klimov, Alex Nichol, Matthias Plappert, Alec Radford, John Schulman, Szymon Sidor, Yuhuai Wu, and Peter Zhokhov. Openai baselines. <https://github.com/openai/baselines>, 2017.
- [15] Benjamin Eysenbach and Sergey Levine. Maximum entropy rl (provably) solves some robust rl problems. *arXiv preprint arXiv:2103.06257*, 2021.
- [16] Scott Fujimoto, Herke van Hoof, and Dave Meger. Addressing function approximation error in actor-critic methods. *arXiv preprint arXiv:1802.09477*, 2018.
- [17] Gauthier Gidel, Tony Jebara, and Simon Lacoste-Julien. Frank-wolfe algorithms for saddle point problems. In *Artificial Intelligence and Statistics*, pages 362–371. PMLR, 2017.
- [18] Ian Goodfellow, Jean Pouget-Abadie, Mehdi Mirza, Bing Xu, David Warde-Farley, Sherjil Ozair, Aaron Courville, and Yoshua Bengio. Generative adversarial nets. In *Advances in neural information processing systems*, pages 2672–2680, 2014.
- [19] Yijie Guo, Junhyuk Oh, Satinder Singh, and Honglak Lee. Generative adversarial self-imitation learning. *arXiv preprint arXiv:1812.00950*, 2018.

- [20] Tuomas Haarnoja, Sehoon Ha, Aurick Zhou, Jie Tan, George Tucker, and Sergey Levine. Learning to walk via deep reinforcement learning. *arXiv preprint arXiv:1812.11103*, 2018.
- [21] Tuomas Haarnoja, Haoran Tang, Pieter Abbeel, and Sergey Levine. Reinforcement learning with deep energy-based policies. *arXiv preprint arXiv:1702.08165*, 2017.
- [22] Tuomas Haarnoja, Aurick Zhou, Pieter Abbeel, and Sergey Levine. Soft actor-critic: Off-policy maximum entropy deep reinforcement learning with a stochastic actor. *arXiv preprint arXiv:1801.01290*, 2018.
- [23] Tuomas Haarnoja, Aurick Zhou, Kristian Hartikainen, George Tucker, Sehoon Ha, Jie Tan, Vikash Kumar, Henry Zhu, Abhishek Gupta, Pieter Abbeel, et al. Soft actor-critic algorithms and applications. *arXiv preprint arXiv:1812.05905*, 2018.
- [24] E Yazdandoost Hamedani, A Jalilzadeh, NS Aybat, and UV Shanbhag. Iteration complexity of randomized primal-dual methods for convex-concave saddle point problems. *arXiv preprint arXiv:1806.04118*, 2018.
- [25] Seungyul Han and Youngchul Sung. Diversity actor-critic: Sample-aware entropy regularization for sample-efficient exploration. *arXiv preprint arXiv:2006.01419*, 2020.
- [26] Elad Hazan, Sham Kakade, Karan Singh, and Abby Van Soest. Provably efficient maximum entropy exploration. In *International Conference on Machine Learning*, pages 2681–2691. PMLR, 2019.
- [27] Zhang-Wei Hong, Tzu-Yun Shann, Shih-Yang Su, Yi-Hsiang Chang, Tsu-Jui Fu, and Chun-Yi Lee. Diversity-driven exploration strategy for deep reinforcement learning. In *Advances in Neural Information Processing Systems*, pages 10489–10500, 2018.
- [28] Rein Houthoofd, Xi Chen, Yan Duan, John Schulman, Filip De Turck, and Pieter Abbeel. Vime: Variational information maximizing exploration. In *Advances in Neural Information Processing Systems*, pages 1109–1117, 2016.
- [29] Shiyu Huang, Hang Su, Jun Zhu, and Ting Chen. Svqn: Sequential variational soft q-learning networks. In *International Conference on Learning Representations*, 2019.
- [30] Sergey Levine and Vladlen Koltun. Guided policy search. In *International Conference on Machine Learning*, pages 1–9, 2013.
- [31] Ya-Feng Liu, Yu-Hong Dai, and Zhi-Quan Luo. Max-min fairness linear transceiver design for a multi-user mimo interference channel. *IEEE Transactions on Signal Processing*, 61(9):2413–2423, 2013.
- [32] Manuel Lopes, Tobias Lang, Marc Toussaint, and Pierre-Yves Oudeyer. Exploration in model-based reinforcement learning by empirically estimating learning progress. In *Advances in neural information processing systems*, pages 206–214, 2012.
- [33] Aleksander Madry, Aleksandar Makelov, Ludwig Schmidt, Dimitris Tsipras, and Adrian Vladu. Towards deep learning models resistant to adversarial attacks. *arXiv preprint arXiv:1706.06083*, 2017.
- [34] Jarryd Martin, Suraj Narayanan Sasikumar, Tom Everitt, and Marcus Hutter. Count-based exploration in feature space for reinforcement learning. *arXiv preprint arXiv:1706.08090*, 2017.
- [35] Bogdan Mazouze, Thang Doan, Audrey Durand, R Devon Hjelm, and Joelle Pineau. Leveraging exploration in off-policy algorithms via normalizing flows. *arXiv preprint arXiv:1905.06893*, 2019.
- [36] Volodymyr Mnih, Koray Kavukcuoglu, David Silver, Andrei A Rusu, Joel Veness, Marc G Bellemare, Alex Graves, Martin Riedmiller, Andreas K Fidjeland, Georg Ostrovski, et al. Human-level control through deep reinforcement learning. *Nature*, 518(7540):529–533, 2015.
- [37] Katta G Murty and Santosh N Kabadi. Some np-complete problems in quadratic and nonlinear programming. Technical report, 1985.

- [38] Ofir Nachum, Mohammad Norouzi, Kelvin Xu, and Dale Schuurmans. Bridging the gap between value and policy based reinforcement learning. In *Advances in Neural Information Processing Systems*, pages 2775–2785, 2017.
- [39] Ofir Nachum, Mohammad Norouzi, Kelvin Xu, and Dale Schuurmans. Trust-pcl: An off-policy trust region method for continuous control. *arXiv preprint arXiv:1707.01891*, 2017.
- [40] Gerhard Neumann et al. Variational inference for policy search in changing situations. In *Proceedings of the 28th International Conference on Machine Learning, ICML 2011*, pages 817–824, 2011.
- [41] Maher Nouiehed, Maziar Sanjabi, Tianjian Huang, Jason D Lee, and Meisam Razaviyayn. Solving a class of non-convex min-max games using iterative first order methods. *arXiv preprint arXiv:1902.08297*, 2019.
- [42] Brendan O’Donoghue, Remi Munos, Koray Kavukcuoglu, and Volodymyr Mnih. Combining policy gradient and q-learning. *arXiv preprint arXiv:1611.01626*, 2016.
- [43] Hassan Rafique, Mingrui Liu, Qihang Lin, and Tianbao Yang. Non-convex min-max optimization: Provable algorithms and applications in machine learning. *arXiv preprint arXiv:1810.02060*, 2018.
- [44] Alexander Rakhlin and Karthik Sridharan. Optimization, learning, and games with predictable sequences. *arXiv preprint arXiv:1311.1869*, 2013.
- [45] Konrad Rawlik, Marc Toussaint, and Sethu Vijayakumar. On stochastic optimal control and reinforcement learning by approximate inference. In *Twenty-Third International Joint Conference on Artificial Intelligence*, 2013.
- [46] John Schulman, Xi Chen, and Pieter Abbeel. Equivalence between policy gradients and soft q-learning. *arXiv preprint arXiv:1704.06440*, 2017.
- [47] John Schulman, Sergey Levine, Pieter Abbeel, Michael Jordan, and Philipp Moritz. Trust region policy optimization. In *Proceedings of the 32nd International Conference on Machine Learning (ICML-15)*, pages 1889–1897, 2015.
- [48] John Schulman, Filip Wolski, Prafulla Dhariwal, Alec Radford, and Oleg Klimov. Proximal policy optimization algorithms. *arXiv preprint arXiv:1707.06347*, 2017.
- [49] Riley Simmons-Edler, Ben Eisner, Daniel Yang, Anthony Bisulco, Eric Mitchell, Sebastian Seung, and Daniel Lee. Qxplore: Q-learning exploration by maximizing temporal difference error. 2019.
- [50] Avi Singh, Larry Yang, Kristian Hartikainen, Chelsea Finn, and Sergey Levine. End-to-end robotic reinforcement learning without reward engineering. *arXiv preprint arXiv:1904.07854*, 2019.
- [51] Emanuel Todorov. General duality between optimal control and estimation. In *2008 47th IEEE Conference on Decision and Control*, pages 4286–4292. IEEE, 2008.
- [52] Emanuel Todorov, Tom Erez, and Yuval Tassa. Mujoco: A physics engine for model-based control. In *Intelligent Robots and Systems (IROS), 2012 IEEE/RSJ International Conference on*, pages 5026–5033. IEEE, 2012.
- [53] Marc Toussaint. Robot trajectory optimization using approximate inference. In *Proceedings of the 26th annual international conference on machine learning*, pages 1049–1056. ACM, 2009.
- [54] Hoi-To Wai, Mingyi Hong, Zhuoran Yang, Zhaoran Wang, and Kexin Tang. Variance reduced policy evaluation with smooth function approximation. *Advances in Neural Information Processing Systems*, 32:5784–5795, 2019.
- [55] Christopher JCH Watkins and Peter Dayan. Q-learning. *Machine Learning*, 8(3):279–292, 1992.

- [56] Brian Hu Zhang, Blake Lemoine, and Margaret Mitchell. Mitigating unwanted biases with adversarial learning. In *Proceedings of the 2018 AAAI/ACM Conference on AI, Ethics, and Society*, pages 335–340, 2018.
- [57] Zeyu Zheng, Junhyuk Oh, and Satinder Singh. On learning intrinsic rewards for policy gradient methods. In *Advances in Neural Information Processing Systems*, pages 4644–4654, 2018.
- [58] Brian D Ziebart, Andrew Maas, J Andrew Bagnell, and Anind K Dey. Maximum entropy inverse reinforcement learning. 2008.

A Detailed Implementation and Algorithm for Max-Min Ent RL

Here, we provide the detailed implementation and algorithm of MME proposed in Section 5.

A.1 Detailed Implementation of MME

First, we consider the vanilla MME proposed in Section 5.2. We approximate the policy π , the reversed action value function Q_R , and the reversed state value function V_R by using deep neural networks with parameters θ , ϕ , and ψ , respectively. Based on the policy update of MME in (9), we define the practical objective function $\hat{J}_\pi(\theta)$ for the parameterized policy π_θ , given by

$$\hat{J}_\pi(\theta) = \mathbb{E}_{s_t \sim \mathcal{D}, a_t \sim \pi_\theta(\cdot|s_t)} [Q_{R,\phi}(s_t, a_t) - \alpha_\pi \log \pi_\theta(a_t|s_t)]. \quad (\text{A.12})$$

Furthermore, based on the Bellman operator \mathcal{T}_R^π in (8), we define the practical loss functions $\hat{L}_{Q_R}(\phi)$ and $\hat{L}_{V_R}(\psi)$ for the parameterized reversed value functions $Q_{R,\phi}$ and $V_{R,\psi}$, respectively, given by

$$\hat{L}_{Q_R}(\phi) = \mathbb{E}_{(s_t, a_t) \sim \mathcal{D}} \left[\frac{1}{2} (Q_{R,\phi}(s_t, a_t) - \hat{Q}(s_t, a_t))^2 \right], \quad (\text{A.13})$$

$$\hat{L}_{V_R}(\psi) = \mathbb{E}_{(s_t, a_t) \sim \mathcal{D}} \left[\frac{1}{2} (V_{R,\psi}(s_t) - \hat{V}(s_t))^2 \right], \quad (\text{A.14})$$

where the target values \hat{Q} and \hat{V} are defined as

$$\hat{Q}(s_t, a_t) = r_t + \gamma \mathbb{E}_{s_{t+1} \sim P(\cdot|s_t, a_t)} [V_{R,\bar{\psi}}(s_{t+1})], \quad (\text{A.15})$$

$$\hat{V}(s_t) = \mathbb{E}_{a_t \sim \pi_\theta(\cdot|s_t)} [Q_{R,\phi}(s_t, a_t) + \alpha_Q \log \pi_\theta(a_t|s_t)]. \quad (\text{A.16})$$

For implementation, we divide r_t by α_π (scaling reward by $1/\alpha_\pi$) in (A.15) instead of multiplying α_π by $\log \pi_\theta$ in (A.12), similarly to the implementation of SAC [22]. $\bar{\psi}$ denotes the neural network parameter of the target value $V_{\bar{\psi}}$ for stable learning, and it is updated by exponential moving average (EMA) of ψ [36].

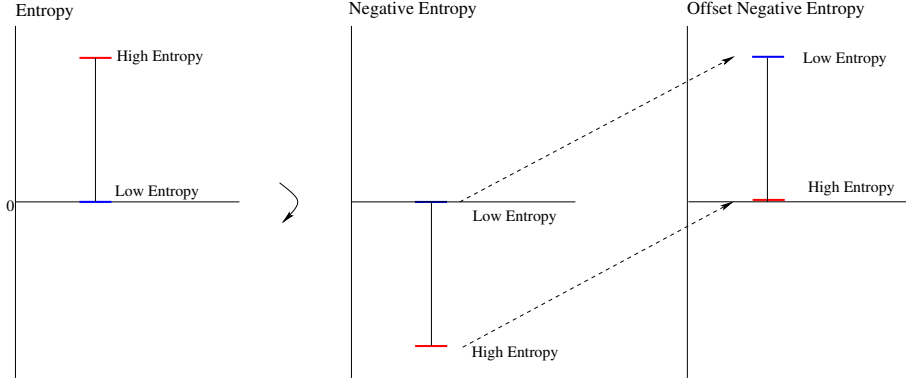


Figure A.1: Offset Negative Entropy

Note that in the reversed value function (A.16), the negative entropy $\mathbb{E}_{a_t \sim \pi_\theta(\cdot|s_t)} \log \pi_\theta(a_t|s_t)$ is added so that lower entropy states yield higher Q -values. Note that the entropy is not necessarily positive in continuous space, but the policy entropy becomes positive soon due to the entropy maximization term $\mathcal{H}(\pi)$ in the policy update, so the negative entropy becomes negative. Hence, if this negative entropy is directly added to Q , the Q -value can decrease in the early stage of learning since Q -function starts near 0 from the random initialization of Q -function network. Note that MME breaks the feedback loop assuming that Q -function continues to increase, so the decrease of Q -function may result in unpredictable effect on learning. Hence, we add a positive offset to the negative entropy in (A.16) so that the offset negative entropy is positive, as seen in Fig. A.1. We considered two types of positive offset: 1) maximum entropy constant $D_a \log 2$ (because the action space is bounded as $[-1, 1]$) and 2) $-\min_m \log \pi_\theta(a_m|s_m)$ in mini-batch $\{(s_m, a_m), m = 1, \dots, M\}$ sampled from

the buffer. In both cases, the offset negative entropy is positive, but the latter case showed better exploration. Hence, we considered the latter case throughout this paper.

In addition, we considered two Q -functions Q_{R,ϕ_i} , $i = 1, 2$ and the minimum of two Q -functions was used for the policy update in (A.12) to reduce overestimation bias as proposed in [16]. Each Q_{R,ϕ_i} minimizes its own loss function $\hat{L}(\phi_i)$ with the common $V_{R,\psi}$. This technique was also considered in SAC.

A.2 Detailed Implementation of DE-MME

The implementation of the disentangled version of MME (DE-MME) proposed in Section 5.3 is as follows. In DE-MME, we have two policies π_T and π_E parameterized with parameters θ_T and θ_E , respectively. Q_R^π is decomposed into $Q_{R,R}^\pi$ and $Q_{R,E}^\pi$, and $Q_{R,R}^{\pi_T,old}$ and $Q_{R,E}^{\pi_E,old}$ are estimated by two estimate Q -functions $Q_{R,R}$ and $Q_{R,E}$ by using their respective Bellman operators $\mathcal{T}_{R,R}^{\pi_T,old}$ and $\mathcal{T}_{R,E}^{\pi_E,old}$, given by

$$\mathcal{T}_{R,R}^{\pi_T,old} Q_{R,R}(s_t, a_t) = r_t + \mathbb{E}_{s_{t+1} \sim P(\cdot|s_t, a_t)} [V_{R,R}(s_{t+1})] \quad (\text{A.17})$$

$$\mathcal{T}_{R,E}^{\pi_E,old} Q_{R,E}(s_t, a_t) = \mathbb{E}_{s_{t+1} \sim P(\cdot|s_t, a_t)} [V_{R,E}(s_{t+1})], \quad (\text{A.18})$$

where $V_{R,R}(s_t) = \mathbb{E}_{a_t \sim \pi_{T,old}(\cdot|s_t)} [Q_{R,R}(s_t, a_t)]$ and $V_{R,E}(s_t) = \mathbb{E}_{a_t \sim \pi_{E,old}(\cdot|s_t)} [Q_{R,E}(s_t, a_t) + \alpha_Q \log \pi_{E,old}(a_t|s_t)]$. For implementation, we parameterize the value functions $Q_{R,R}$, $V_{R,R}$, $Q_{R,E}$, $V_{R,E}$ by neural network parameters ϕ_R , ψ_R , ϕ_E , ψ_E , respectively. Then, based on the policy updates (11) and (10), we define the objective functions $\hat{J}_{\pi_T}(\theta_T)$ and $\hat{J}_{\pi_E}(\theta_E)$ respectively for the parameterized policies π_{T,θ_T} and π_{E,θ_E} , given by

$$\hat{J}_{\pi_T}(\theta_T) = \mathbb{E}_{s_t \sim \mathcal{D}, a_t \sim \pi_{T,\theta_T}(\cdot|s_t)} [Q_{R,R,\phi_R}(s_t, a_t) + Q_{R,E,\phi_E}(s_t, a_t) - \alpha_\pi \log \pi_{T,\theta_T}(a_t|s_t)], \quad (\text{A.19})$$

$$\hat{J}_{\pi_E}(\theta_E) = \mathbb{E}_{s_t \sim \mathcal{D}, a_t \sim \pi_{E,\theta_E}(\cdot|s_t)} [Q_{R,E,\phi_E}(s_t, a_t) - \alpha_\pi \log \pi_{E,\theta_E}(a_t|s_t)]. \quad (\text{A.20})$$

Based on the Bellman operators (A.17) and (A.18), we define the loss functions $\hat{L}_{Q_{R,R}}(\phi_R)$, $\hat{L}_{V_{R,R}}(\psi_R)$, $\hat{L}_{Q_{R,E}}(\phi_E)$, and $\hat{L}_{V_{R,E}}(\psi_E)$ for the parameterized value functions Q_{R,R,ϕ_R} , V_{R,R,ψ_R} , Q_{R,E,ϕ_E} , and V_{R,E,ψ_E} , respectively, given by

$$\hat{L}_{Q_{R,R}}(\phi_R) = \mathbb{E}_{(s_t, a_t) \sim \mathcal{D}} \left[\frac{1}{2} (Q_{R,R,\phi_R}(s_t, a_t) - \hat{Q}_{R,R}(s_t, a_t))^2 \right], \quad (\text{A.21})$$

$$\hat{L}_{V_{R,R}}(\psi_R) = \mathbb{E}_{(s_t, a_t) \sim \mathcal{D}} \left[\frac{1}{2} (V_{R,R,\psi_R}(s_t) - \hat{V}_{R,R}(s_t))^2 \right], \quad (\text{A.22})$$

$$\hat{L}_{Q_{R,E}}(\phi_E) = \mathbb{E}_{(s_t, a_t) \sim \mathcal{D}} \left[\frac{1}{2} (Q_{R,E,\phi_E}(s_t, a_t) - \hat{Q}_{R,E}(s_t, a_t))^2 \right], \quad (\text{A.23})$$

$$\hat{L}_{V_{R,E}}(\psi_E) = \mathbb{E}_{(s_t, a_t) \sim \mathcal{D}} \left[\frac{1}{2} (V_{R,E,\psi_E}(s_t) - \hat{V}_{R,E}(s_t))^2 \right], \quad (\text{A.24})$$

where the target values $\hat{Q}_{R,R}$, $\hat{V}_{R,R}$, $\hat{Q}_{R,E}$, and $\hat{V}_{R,E}$ are defined as

$$\hat{Q}_{R,R}(s_t, a_t) = r_t + \gamma \mathbb{E}_{s_{t+1} \sim P(\cdot|s_t, a_t)} [V_{R,\bar{\psi}_R}(s_{t+1})], \quad (\text{A.25})$$

$$\hat{V}_{R,R}(s_t) = \mathbb{E}_{a_t \sim \pi_{T,\theta_T}} [Q_{R,R,\phi_R}(s_t, a_t)], \quad (\text{A.26})$$

$$\hat{Q}_{R,E}(s_t, a_t) = \gamma \mathbb{E}_{s_{t+1} \sim P(\cdot|s_t, a_t)} [V_{R,E,\bar{\psi}_E}(s_{t+1})], \quad (\text{A.27})$$

$$\hat{V}_{R,E}(s_t) = \mathbb{E}_{a_t \sim \pi_{E,\theta_E}} [Q_{R,E,\phi_E}(s_t, a_t) + \alpha_Q \log \pi_{E,\theta_E}(a_t|s_t)]. \quad (\text{A.28})$$

Here, $\bar{\psi}_R$ and $\bar{\psi}_E$ are the target network parameters and we consider Q -functions $Q_{R,R,\phi_{R,i}}$, $i = 1, 2$ for $Q_{R,R}$ and $Q_{R,E,\phi_{E,i}}$, $i = 1, 2$ for $Q_{R,E}$.

Other details are the same as those in the implementation of vanilla MME. We summarize the propose algorithm in Algorithm 1.

Algorithm 1 (Disentangled) Max-Min Entropy RL

```
if Disentangled then
  Initialize  $\theta_T, \theta_E, \psi_R, \bar{\psi}_R, \psi_E, \bar{\psi}_E, \phi_{R,i}, \phi_{E,i}, i = 1, 2$ 
else
  Initialize  $\theta, \psi, \bar{\psi}, \phi_i, i = 1, 2$ 
end if
for each iteration do
  Sample a trajectory  $\tau$  from the behaviour policy and store  $\tau$  in the buffer  $\mathcal{D}$ 
  for each gradient step do
    Sample a random mini-batch of size  $M$  from  $\mathcal{D}$ 
    if Disentangled then
      Compute  $\hat{J}_{\pi_T}(\theta_T), \hat{L}_{Q_{R,R}}(\phi_{R,i}), \hat{L}_{V_{R,R}}(\psi_R)$  from the mini-batch
      Compute  $\hat{J}_{\pi_E}(\theta_E), \hat{L}_{Q_{R,E}}(\phi_{E,i}), \hat{L}_{V_{R,E}}(\psi_E)$  from the mini-batch
       $\theta_T \leftarrow \theta_T + \delta \nabla_{\theta_T} \hat{J}_{\pi_T}(\theta_T), \theta_E \leftarrow \theta_E + \delta \nabla_{\theta_E} \hat{J}_{\pi_E}(\theta_E)$ 
       $\psi_R \leftarrow \psi_R - \delta \nabla_{\psi_R} \hat{L}_{V_{R,R}}(\psi_R), \psi_E \leftarrow \psi_E - \delta \nabla_{\psi_E} \hat{L}_{V_{R,E}}(\psi_E)$ 
       $\phi_{R,i} \leftarrow \phi_{R,i} - \delta \nabla_{\phi_{R,i}} \hat{L}_{Q_{R,R}}(\phi_{R,i}), \phi_{E,i} \leftarrow \phi_{E,i} - \delta \nabla_{\phi_{E,i}} \hat{L}_{Q_{R,E}}(\phi_{E,i}), i = 1, 2$ 
      Update  $\bar{\psi}_E, \bar{\psi}_R$  by EMA from  $\psi_E, \psi_R$ , respectively
    else
      Compute  $\hat{J}_{\pi}(\theta), \hat{L}_Q(\phi_i), \hat{L}_V(\psi)$  from the mini-batch
       $\theta \leftarrow \theta + \delta \nabla_{\theta} \hat{J}_{\pi}(\theta)$ 
       $\psi \leftarrow \psi - \delta \nabla_{\psi} \hat{L}_V(\psi)$ 
       $\phi_i \leftarrow \phi_i - \delta \nabla_{\phi_i} \hat{L}_Q(\phi_i), i = 1, 2$ 
      Update  $\bar{\psi}$  by EMA from  $\psi$ 
    end if
  end for
end for
```

B Experimental Setup

Here is the detailed setup for the overall experiments considered in this paper. Table B.1 shows the hyperparameter setup of MME and SAC. Basically, we follow the hyperparameter setup in the SAC paper [22] for the parameters common to SAC and MME. Here, squashed Gaussian for the policy distribution means that the Gaussian policy is squashed into $[-1, 1]$ by a tanh layer because we consider environments with bounded action space as proposed in [22]. Table B.2 shows the detailed setup for all the considered environments in this paper. For the policy entropy coefficient α_{π} in Table B.2, we considered the entropy coefficient value proposed in [22, 25] for each task, and used the common α_{π} ($\alpha = \alpha_{\pi}$ for SAC), MME, and DE-MME. In addition, the value entropy coefficient α_Q in Table B.2 was chosen as the best performing value among $\alpha_Q \in \{0.1, 0.2, 0.5, 1, 2, 5, 10\}$ for each task. For more details, please refer to ablation studies on the entropy coefficients α_{π} and α_Q in Appendix D. For SparseMujoco tasks, the agent gets reward 1 if it exceeds the x -axis threshold τ in Table B.2, and for DelayedMujoco tasks, rewards are accumulated for D time steps in Table B.2 and the agent gets the accumulated reward, as stated in Section 6.2. We conducted all experiments in Section 6 in environments where only CPUs are used without GPU. We used Mujoco and OpenAI Gym. We purchased a Mujoco license. OpenAI Gym is MIT license that allows use, copy, modification, merge, etc. So, it does cause any issue. The source code of the SAC baseline is open to public (MIT license), so using it does not have any issues. We did not use any data which contains personally identifiable information or offensive contents.

	SAC	MME/DE-MME
Discount factor γ	0.999 for pure exploration / 0.99 for rewarded setup	
Learning rate δ	$3 \cdot 10^{-4}$	
Episode length N	1000	
Mini-batch size M	256	
Replay buffer size	10^6	
Smoothing coefficient for EMA	0.005	
Optimizer	Adam	
Num. of hidden layers	2	
Size of hidden layers	256	
Activation layer	ReLU	
Output layer	Linear	
Policy distribution	Squashed Gaussian distribution	

Table B.1: Common hyperparameter setup

	State dim.	Action dim.	α_π (α for SAC)	α_Q (MME)	α_Q (DE-MME)	
ContinuousMaze	2	2	1	0.5	.	
HumanoidStandup-v1	376	17	1	2.0	0.1	
Humanoid-v1	376	17	0.05	1.0	1.0	
	State dim.	Action dim.	α_π	α_Q (MME)	α_Q (DE-MME)	Threshold τ
SparseHopper-v1	11	3	0.04	1.0	2.0	1.0
SparseHalfCheetah-v1	17	6	0.02	2.0	2.0	5.0
SparseWalker2d-v1	17	6	0.02	0.5	2.0	1.0
SparseAnt-v1	111	8	0.01	0.2	0.1	1.0
	State dim.	Action dim.	α_π	α_Q (MME)	α_Q (DE-MME)	Delay D
Del.Hopper-v1	11	3	0.2	1.0	2.0	20
Del.HalfCheetah-v1	17	6	0.2	2.0	2.0	20
Del.Walker2d-v1	17	6	0.2	0.5	2.0	20
Del.Ant-v1	111	8	0.2	0.2	0.1	20

Table B.2: Detailed setup for environments

C Additional Results on Performance Comparisons

Here, we provide the max average return table of MME/DE-MME and SAC for experiments on sparse-rewarded tasks in Section C.1. In addition, we provide detailed explanation, implementation, and the result plots for performance comparison to recent exploration methods in Section C.2 and general RL algorithms in Section C.3.

C.1 Max Average Return Results for Performance Comparison to SAC

Table C.1 shows the max average return performance of MME/DE-MME and SAC on sparse-reward (SparseMujoco and DelyaedMujoco) tasks in Section 6.2. The value following the \pm sign in the table means one standard deviation of the max average return, and the best result among the algorithms for each task is shown in bold. For all the considered tasks, both MME/DE-MME have the better max average return performance than SAC, and DE-MME has the best performance in most cases. Note that this result is consistent with the results shown in Figs. 5 and 6.

	MME	DE-MME	SAC
Sps.Hopper	902.50±4.36	893.30±6.72	823.70±215.35
Sps.HalfCheetah	903.50±34.97	924.90±39.57	386.90±404.70
Sps.Walker2d	818.00±208.60	886.60±25.77	273.30±417.51
Sps.Ant	953.70±28.39	973.60±12.55	963.80±42.51
Del. Hopper	3421.32±88.29	3435.28±39.55	2175.31±1358.39
Del. HalfCheetah	7299.28±1562.19	8451.20±1375.27	3742.33±3064.55
Del. Walker2d	5148.58±193.78	5274.89±186.35	3220.92±1107.91
Del. Ant	4664.04±836.37	4851.64±830.88	3248.43±1454.48

Table C.1: Max average return of MME/DE-MME and SAC

C.2 Comparison to Recent Exploration Methods on Sparse-Rewarded Tasks

In Section 6.2, we compared the performance of MME/DE-MME with various recent exploration methods on the considered sparse-rewarded Mujoco tasks. For comparison, we considered two types of exploration methods: action-based exploration that modifies the policy distribution itself to enhance exploration, and state-based exploration that finds rare states for better exploration. We first describe the detailed explanation and implementation for the considered recent exploration methods.

For action-based exploration methods, we considered 1) SAC with divergence regularization [27] (SAC-Div), which adds a single diversity term $\alpha_d D(\pi||q)$ to the SAC objective for some divergence D between the policy π and the sample action distribution q to choose actions away from the actions in the buffer and 2) diversity actor-critic [25] (DAC), which regularizes sample-aware entropy $\alpha \mathcal{H}(\beta\pi + (1 - \beta)q)$, $\beta \in (0, 1)$ instead of the policy entropy $\alpha \mathcal{H}(\pi)$ of SAC to enhance the policy entropy while the policy chooses actions to avoid the previously sampled actions in the buffer. For SAC-Div, we considered the KL divergence for D and the adaptive scaling of α_d with scaling parameter $\delta_d = 0.2$, as suggested in [27]. For DAC, we used the same α with the SAC baseline, and $\beta = 0.5$ for SparseMujoco tasks and the adaptive β with control hyperparameter $c_{\text{adapt}} = -2.0 \dim(\mathcal{A})$ for DelayedMujoco tasks, as suggested in [25].

For state-based exploration methods, we considered 1) random network distillation [9] (RND), which uses the model prediction error $\|f(s_{t+1}) - f_t(s_{t+1})\|^2$ as an intrinsic reward $r_{\text{int},t}$ to search for rare states, where f_s is a predictor network and f_t is a randomly fixed target network, and 2) MaxEnt(State) [26] which maximizes the entropy of state mixture distribution $\mathcal{H}(d^{\pi_{\text{mix}}})$ for maximizing $\mathcal{H}(d^\pi)$ to visit states uniformly, where d^π is the state distribution induced by the policy π . MaxEnt(State) is Originally proposed for pure exploration, but we used the reward of MaxEnt(State) $-\log(d^{\pi_{\text{mix}}}(s) + c_s)$ as an intrinsic reward to search for rare states as the RND case for comparison on sparse-rewarded tasks, where c_s is the smoothing constant in [26]. Then, the reward becomes $r_t = r_{\text{ext},t} + c_{\text{int}} r_{\text{int},t}$, where $r_{\text{ext},t}$ is the external reward from the environment and $c_{\text{int}} > 0$ is the intrinsic reward coefficient. For RND, we used MLP with 2 ReLU hidden layers of size 256 and linear output layer of size 20 for both predictor and target networks, and the intrinsic reward coefficient $c_{\text{int}} = 5$ for sparse-rewarded Ant/HalfCheetah tasks and $c_{\text{int}} = 10$ for sparse-rewarded Hopper/Walker tasks, properly chosen from $\{1, 2, 5, 10\}$. For MaxEnt, we computed $d^{\pi_{\text{mix}}}$ based on projection/Kernel density estimation with Epanechnikov kernel using 100k previous states stored in the buffer, and used the intrinsic reward coefficient $c_{\text{int}} = 0.01$ for sparse-rewarded Ant/HalfCheetah tasks and $c_{\text{int}} = 0.02$ for sparse-rewarded Hopper/Walker tasks, properly chosen from $\{0.01, 0.02, 0.05, 0.1\}$. For state-based exploration methods, we used the Gaussian policy with fixed standard deviation $\sigma = 0.3$, and the other implementation setup was the same with the SAC baseline to make fair comparison between action-based and state-based exploration methods.

Fig. C.1 shows the corresponding average return performance on SparseMujoco tasks and Delayed-Mujoco tasks. It is seen that proposed MME and DE-MME perform best in most of the considered tasks.

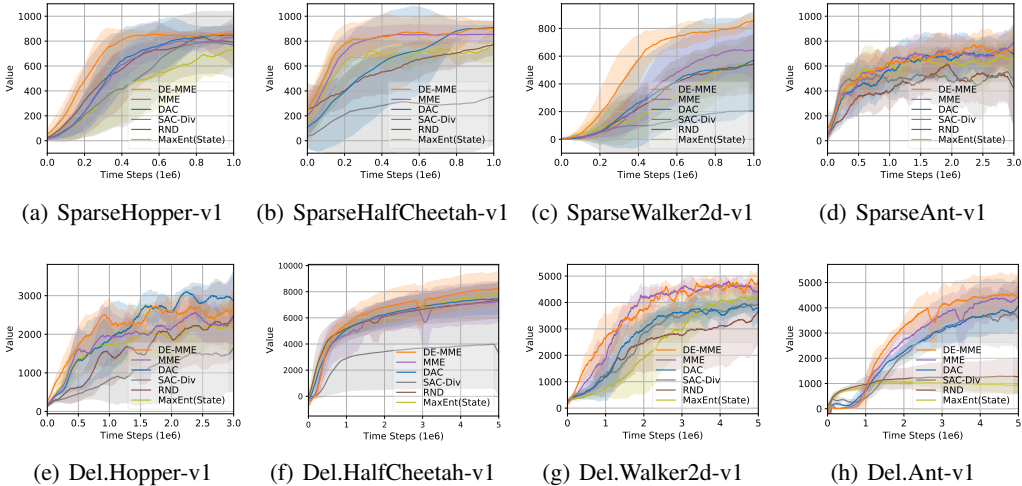


Figure C.1: Performance comparison to recent exploration methods on sparse-rewarded Mujoco tasks

C.3 Comparison to Recent General RL Algorithms on Dense-Rewarded Tasks

In Section 6.2, we compared the performance of MME/DE-MME with various recent on-policy and off-policy RL algorithms on high action-dimensional dense-rewarded (original) Mujoco tasks (Humanoid, HumanoidStandup). The considered recent algorithms are as follows. For on-policy RL, we considered trust region policy optimization (TRPO) [39], which has a KL divergence constraint to guarantee the monotone improvement in policy gradient update, and proximal policy optimization (PPO) [48], which efficiently restricts the amount of policy update by clipping the importance sampling ratio for stable learning. For both algorithms, we used implementations in the OpenAI baselines [14].

For off-policy RL, we considered two RL algorithms based on maximum entropy RL: soft actor-critic (SAC) [22] explained in detail in Section 3.2, and soft Q-learning (SQL) [21], which represents the policy with an energy-based model, where the energy function is the Q -function and uses Stein variational gradient descent to learn the sampling network. For both algorithms, we used the implementations in authors' Github: <https://github.com/haarnoja/sac> for SAC and <https://github.com/haarnoja/softqlearning> for SQL.

Fig. C.2 shows the corresponding average return performance on Humanoid and HumanoidStandup tasks. It is seen that proposed MME and DE-MME yield superior performance to other RL algorithms for both tasks. Hence, we can observe that the proposed method is superior not only in sparse-reward environments but also in difficult dense-reward environments.

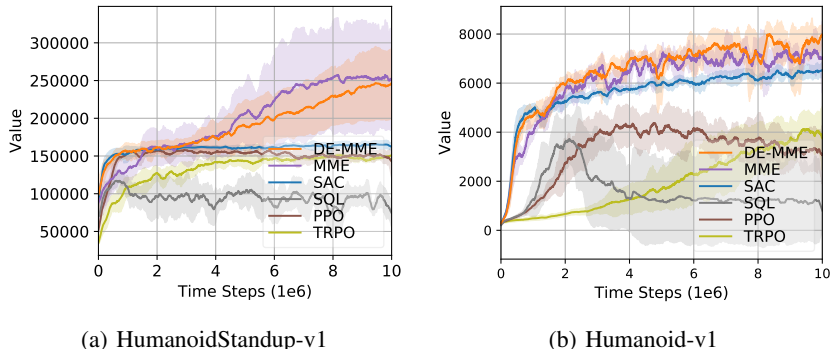


Figure C.2: Performance comparison to general RL algorithms on dense-rewarded Mujoco tasks

D Ablation Studies

In this section of Appendix, we provide detailed ablation studies on the DelayedHalfCheetah task. For the hyperparameters not mentioned separately in each study, we used the hyperparameter setup in Table B.2 by default.

First, Figs. D.1(a) and D.1(b) show the mean number of state visitation and the corresponding performance, respectively, for MME/DE-MME with $\alpha_Q = 2.0$ and SAC. Then, in order to see how α_Q and α_π affect the performance of DE-MME, we performed the same experiment with varying α_Q and α_π , and the results are shown in Figs. D.1(c) and D.1(d).

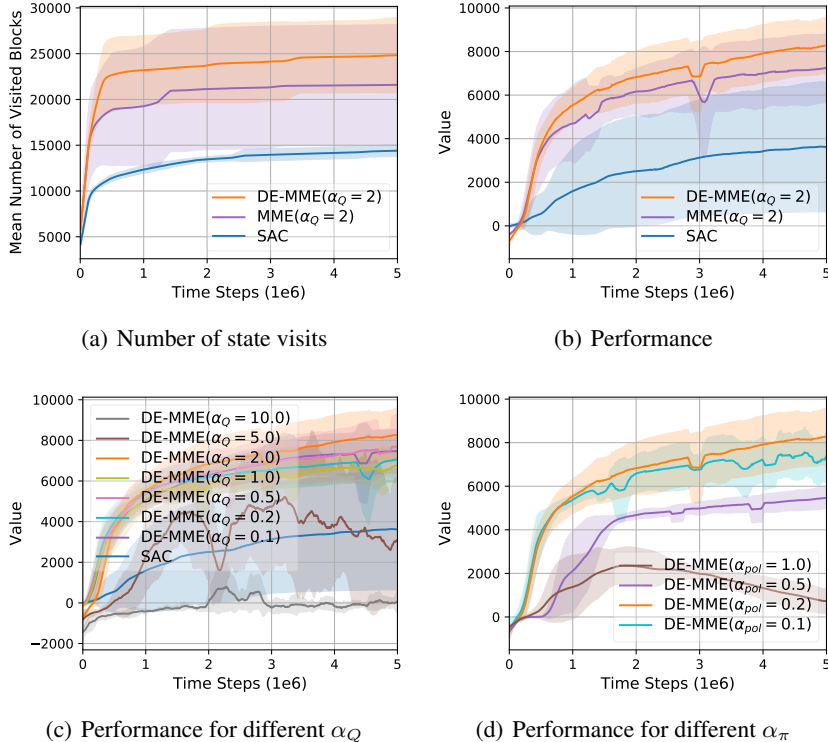


Figure D.1: Ablation studies on DelayedHalfCheetah task

MME vs. DE-MME: Fig. D.1(a) shows the average number of quantized state visitation of MME/DE-MME and SAC. As in the pure exploration case, MME/DE-MME visit much more states than SAC, which shows the superior exploration performance of MME/DE-MME to SAC even in environments with reward. As mentioned in Section 2, enhanced exploration can help the policy not fall into a local optimum and converge better, and lead better final performance in various sparse-rewarded tasks, as shown in Fig. D.1(b). It is also seen that DE-MME visits more states and has better performance than MME with the same α_Q . This shows that the disentangling exploration from exploitation proposed in Section 5.3 is indeed helpful for better exploration and performance.

Value entropy coefficient α_Q : The value entropy coefficient α_Q is one of the most important hyperparameters for MME/DE-MME, which determines the rate of change in the Q -function as the policy entropy changes. Thus, it affects the exploration from the Q -function to visit states with low entropy, as seen in Fig. 3(a) in the main paper. In tasks with reward, α_Q controls the ratio between the impacts of the reward function and the policy entropy on the Q -function in the policy updates (9) and (11). If α_Q is too large, the impact of the policy entropy becomes too dominant compared that of the reward function, and this adversely affects the performance, as seen in Fig. D.1(c). On the other hand, if α_Q is too small, the impact of the Q -function to visit states with low policy entropy for better exploration is reduced, so the performance again deteriorates, as seen in Fig. D.1(c). As a result, there is a trade-off between the reward function and the policy entropy in the Q -function, and we found that $\alpha_Q = 2.0$ worked best for the DelayedHalfCheetah task.

Policy entropy coefficient α_π : Whereas the value entropy coefficient α_Q controls the entropy impact inside the Q -function to visit states with low entropy, the policy entropy coefficient α_π controls the ratio of Q -function itself to the policy entropy term to actually increase the policy entropy for given state in the policy updates (9) or (11). If α_π is too large, the policy dominantly increases its entropy rather than increasing the expectation of Q -function including the reward sum in the policy update, so the performance deteriorates, as seen in Fig. D.1(d). If α_π is too small, on the other hand, then the policy is updated almost exclusively by the Q -function, so it is difficult to increase its entropy and results in poor performance, as seen in Fig. D.1(d). We observed that $\alpha_\pi = 0.2$ worked best for the DelayedHalfCheetah task. From the ablation studies, we conclude that it is important to choose appropriate α_Q and α_π to control the balance among the reward, the Q -function and the policy entropy.

E Answers to the Checklist

E.1 Limitations of Our Works

As explained in Section 4, SAC theoretically guarantees the optimal convergence for maximum entropy RL framework in finite MDP setup, but it shows the saturation problem in practical situation with function approximation and sample-based on learning when it learns the pure exploration task. In order to overcome this limitation, we proposed Max-Min entropy (MME) RL, which learns Q -function to explore states with low entropy and breaks the feedback loop of maximum entropy SAC that causes saturation.

Although the proposed MME framework shows excellent performance compared to previous maximum entropy algorithms, we do not have proof of convergence for MME at this point even for finite MDPs. This theoretical work remains as a future work. Another issue is the complexity of MME. The complexity of DE-MME is larger than SAC since it has more parameters to learn than SAC. As a result, learning time can increase slightly compared to SAC. However, most RL algorithms consider sample complexity most important, and DE-MME has superior performance to MME or SAC. Thus, we think that the increased complexity of DE-MME is well justified due to its superior performance.